IEEE Photonics Journal
An IEEE Photonics Society Publication

Open Access

# A Double-Cladding Single Polarization Photonic Crystal Fiber and Its Structure Deviation Tolerance

Volume 10, Number 6, December 2018

Yating Shen
Longfei Wang
Meisong Liao
Yinyao Liu
Fei Yu
Dakun Wu
Wanjun Bi
Yongzheng Fang
Weiqing Gao

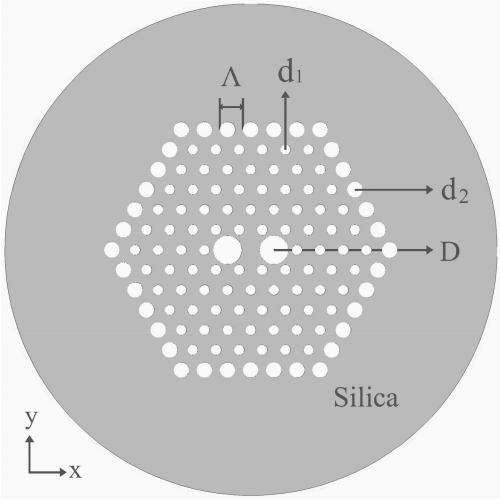


DOI: 10.1109/JPHOT.2018.2882462
1943-0655 © 2018 IEEE

IEEE photonics SOCIETY

IEEE

# A Double-Cladding Single Polarization Photonic Crystal Fiber and Its Structure Deviation Tolerance

**Yating Shen,[1,2] Longfei Wang,[1] Meisong Liao,[1] Yinyao Liu,[1] Fei Yu,[1] Dakun Wu,[1,2] Wanjun Bi,[1,2] Yongzheng Fang,[3] and Weiqing Gao[4]**

[1]Laboratory of High Power Laser Components, Shanghai Institute of Optics and Fine Mechanics, Shanghai 201800, China
[2]University of Chinese Academy of Sciences, Beijing 100049, China
[3]Shanghai Institute of Technology, Shanghai 201418, China
[4]School of Electronic Science and Applied Physics, Hefei University of Technology, Hefei 230009, China

*DOI:10.1109/JPHOT.2018.2882462*


Manuscript received September 18, 2018; accepted November 15, 2018. Date of publication November 21, 2018; date of current version December 14, 2018. This work was supported by the National Key Research and Development Program of China (2018YFB0504500), by the National Natural Science Foundation of China (NSFC) (61475171, 61875052, 61705244, 61307056), by the Natural Science Foundation of Shanghai (17ZR1433900, 17ZR1434200), and by the CAS Pioneer Hundred Talents Program. Corresponding author: Meisong Liao (e-mail: liaomeisong@siom.ac.cn).

**Abstract:** We propose a novel broadband single-polarization single-mode (SPSM) photonic crystal fiber with hexagonally latticed circular airholes. Combined with our fabricated polarization maintaining fiber, it has demonstrated that the enlarged air holes in the outmost layer are superior for the confinement loss reduction. At the optimized parameters, the wavelength of SPSM region ranges from 1.52 to 2.13 μm, where only y-polarized fundamental mode exists and the confinement loss is 0.051 dB/km at 1.55 μm. The influence of realistic fabrication errors involving structure deviation on SPSM operation has also been systematically investigated.

**Index Terms:** Fiber design and fabrication, photonic crystal fibers, single-polarization single mode, fiber properties

## 1. Introduction

Single-polarization single-mode (SPSM) fiber supports only one polarization state of fundamental modes over a specific wavelength range, which is also known as absolute single-polarization fiber [1], [2]. Owing to its unique properties of eliminating polarization crosstalk effect and preventing the polarization-mode dispersion, this fiber has extensive applications in fiber optic gyroscopes, high-speed transmission systems and other polarization-sensitive components [3], [4].

To achieve SPSM operation, a high birefringence is essential for the optical fiber to separate the two orthogonally polarized fundamental modes [5]. In the last few years, the photonic crystal fiber (PCF) as a new type of media has been preferred to obtain broadband SPSM guidance [6], [7], since its high index contrast between silica and air account for an appreciably high birefringence. Numerous designs have involved broadband SPSM guidance in PCFs. Several SPSM-PCFs evolved

from traditional PM-PCF (PM1550-01, by NKT Photonics) have been proposed [8], [9]. To further broaden operation bandwidth, another kind of strategy is through exploiting elliptical air-holes and rectangular-lattice [10], [11]. In spite of the revealed attractive features of these designs, the huge challenge lies in the fabrication of these above-mentioned PCFs. Also, it is well known from recent studies [12], [13], the modes in the fiber are inherently leaky since the number of air holes in the cladding is finite. The confinement loss can be reduced to the desirable level by increasing the number of air rings [14], [15], but it still increases the complexity of fabrication. Furthermore, fibers with a noted length are preferred in the application concerning gyroscope, in which case a tiny structure deviation can even accumulate to a remarkable performance deviation, leading to a consequently urged research on structure tolerance. Current studies have demonstrated that dimension variations of SPSM fiber have a strong influence on the performance of SPSM operation [16], [17]. However, the analysis of air holes deviating from their original positions has still been neglected.

In this paper, a double-cladding PM-PCF with hexagonally latticed circular airholes is reported on, which is fabricated in our lab using the stack-and-draw method [18], [19]. A low confinement loss of $3.06 \times 10^{-3}$ dB/km and a birefringence of $3.87 \times 10^{-4}$ at 1.55 μm are obtained, theoretically. Based on the double-cladding method, we propose a novel broadband single-polarization single-mode PCF with six rings of circular airholes arranged in hexagonal lattice. It is confirmed from numerical results that a low confinement loss (LCL) bandwidth of 260 nm for SPSM operation including the wavelength of 1.55 μm has been achieved. Moreover, a research covering structure deviation tolerance has been laid emphasis on so as to well analyze the fiber properties, which is one of the key issues of the SPSM fiber.

## 2. Experiments

Here, we present a simple double-cladding polarization maintaining PCF designed to deliver polarized light. This PM-PCF was fabricated using the stack and draw technique commonly used for photonic crystal fiber fabrication. Fig. 1 shows the fabrication process of our PM-PCF. The first process was to draw numbers of silica capillaries and rods. Then, the fabricated capillaries were sealed at one single end and stacked in a hexagonal shape, as shown in Fig. 1(b). Stacked capillaries were inserted into a suitable jacketing tube, and voids at six hexagonal sides were filled with packing rods of different sizes. In our design, the center capillary was replaced with a rod of the same size as the other capillaries. Two capillaries near the core rod and capillaries in the fifth ring were all replaced with larger inner hole capillaries. After that, the PCF perform was prepared and drawn to the fiber.

## 3. Results and Discussion

### 3.1 Characteristic of Fabricated PM-PCF

A microscope image of the PM-PCF fabricated in pure silica is shown in the Fig. 2(a), with x denoting the fast axis and y denoting slow axis. It consists of five periods of air holes, appearing as the black area in the Fig. 2(a). The pure silica has been utilized as the background whose chromatic dispersion was determined by the Sellmeier equation [20]. The confinement loss [1] can be expressed as

$$CL = 8.686 \times \frac{2\pi}{\lambda} \mathrm{Im}[n_{eff}] \times 10^{-3}$$

where $n_{eff}$ is the effective refractive index, Im stands for the imaginary part, the unit of $CL$ and the wavelength of $\lambda$ are dB/km and meter, respectively. Simulation of PM-PCF was performed using by the full vector finite element method with perfectly matched layers [6].

From the measurement, the outer diameter PCF is 124 μm, the pitch size is 6.78 μm, and a variety of surrounded airhole with three different values are obtained. Two large air holes adjacent

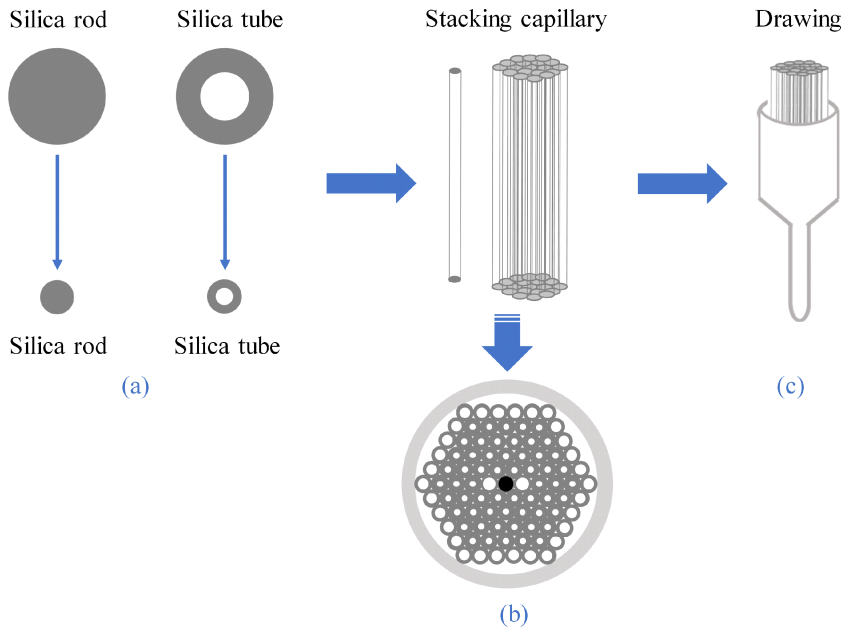


Fig. 1. Schematic of the fabrication process of PM-PCF. (a) Drawing 1 mm silica capillaries and different size rods. (b) Stacking capillaries based on a hexagonal lattice. (c) Fiber drawing process.

to the core have a diameter of 8.11 μm. The big holes distributed in the fifth ring have a diameter of 4.09 μm and other small air hole diameters are 3.22 μm. Fig. 2(a) has been imported directly into software and simulated. Two orthogonal polarized fundamental modes were found, corresponding to Fig. 2(b) and Fig. 2(c). The effective refractive indexes for two polarization modes are 1.435957 and 1.436344, independently, showing a birefringence of $3.87 \times 10^{-4}$ at 1.55 μm. The calculated confinement loss corresponding to x- and y-polarization are $3.06 \times 10^{-3}$ dB/km and $1.56 \times 10^{-4}$ dB/km, respectively. In Fig. 2(a), it has been found a defect hole with a smaller size at the right-down corner in the outmost layer, causing a slight increasement in the confinement loss compared to that of ideal mode - the y-polarization is only $3.94 \times 10^{-5}$ dB/km. On the other hand, given the air hole of the fifth layer is shrunken to 2.5 μm, the confinement loss of y-polarized mode will be dramatically increased to 7.78 dB/km. To draw a point home, the enlarged air holes in the outermost ring can effectively reduce the loss by at least two orders of magnitude, compared to the case where air holes are set as small or shrunken ones. At the same time, based on this double-cladding method, a broadband SPSM-PCF can be realized through adjusting structure parameters of the fiber.

### *3.2 Structural Optimization of PM-PCF*

There are two design principles to obtain SPSM-PCFs [21]. The first one is based on eliminating the unwanted polarized mode through its resonance coupling to the cladding defect modes, named as index-matching coupling method [22]. The second method is through exploiting the asymmetry in the fiber core and/or cladding region to make the effective refractive index of one polarization state of the fundamental mode lower than fundamental space-filling mode (FSM), which is called deadline method [23]. In this letter, the second technique is adopted to achieve SPSM-PCF.

As shown in Fig. 3, the proposed single-polarization single-mode PCF with a hexagon-lattice arrangement is composed of six rings of circular air holes with the outermost cladding formed by big air holes. The schematic design of SPSM-PCF is based on traditional PM-PCF, where two large air holes and four small air holes in the first ring of the cladding together form an anisotropic core area. The diameter of large air holes in the core region is D. The pitch of two adjacent air holes is $\Lambda$. The diameter of the inner cladding air holes is $d_1$ and the diameter of air hole in the outermost

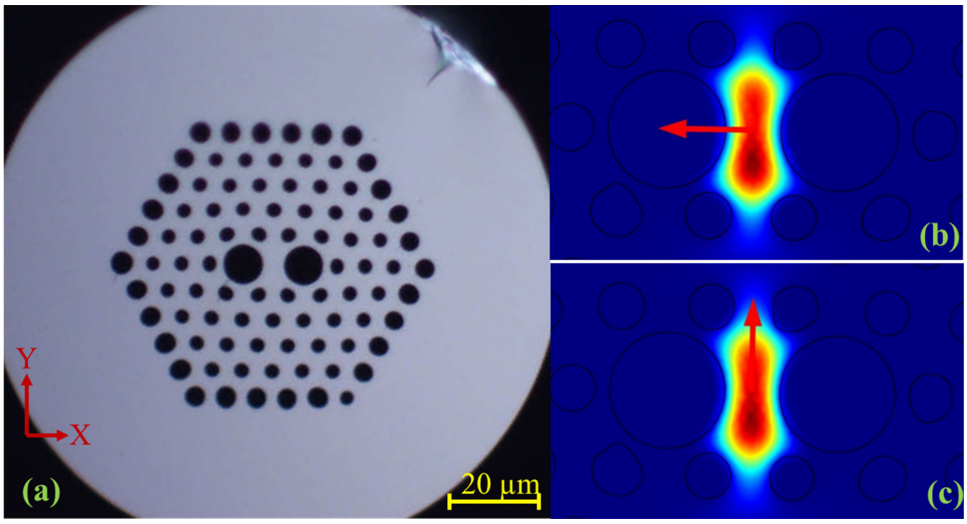


Fig. 2. Microscope image of PM-PCF (a) and simulated intensity profile of (b) x-polarized mode and (c) y-polarized mode.

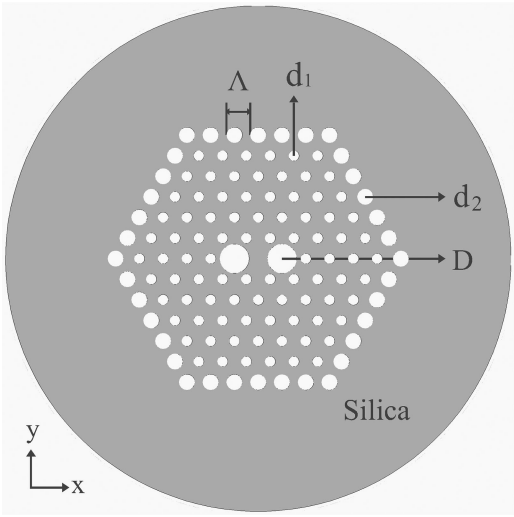


Fig. 3. Cross section of the proposed SPSM-PCF.

ring is $d_2$. In our calculation, $\Lambda = 3$ μm, D = 3.8 μm, $d_1 = 1.5$ μm, and the value of $d_2$ is adjusted to optimize the polarization property.

The design of SPSM-PCF operation is aimed at the wavelength of 1.55 μm. Fig. 4(a) shows the birefringence and confinement loss of x- and y-polarized modes at a target wavelength $\lambda = 1.55$ μm as a function of $d_2$. The confinement loss monotonically decreases while the birefringence tends to flatten as the value of $d_2$ increases, indicating that the design can effectively reduce the loss without affecting its birefringence performance. The band of low confinement loss for SPSM operation (LCL-SPSM) as defined in [24] is the wavelength range over which one polarization state is attenuated by at least 25 dB/km while the orthogonal state suffers less than 1 dB/km. Calculation was performed in 0.1 μm steep, and it is found that when $d_2 = 2.2$ μm, the confinement loss of x- and y- polarized modes are 91.43 dB/km and 0.051 dB/km, which can ensure not only the x polarization mode leak out but also the confinement loss of y polarization mode be low enough. The layers dependence of the confinement loss with normal sized air holes is detailed in Fig. 4(b), as expected, the 10 rings provide a better confinement of lightwave than the 6 rings. Compared

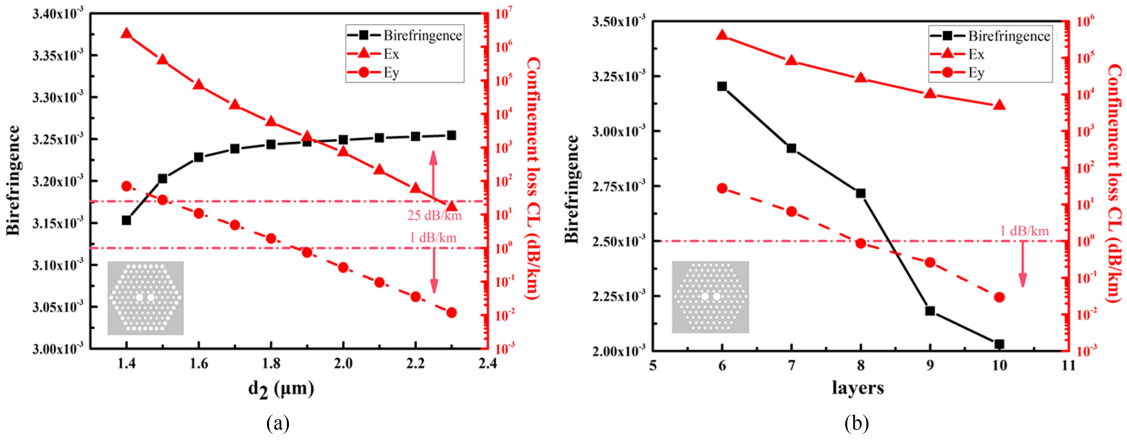


Fig. 4. Birefringence and confinement loss of x- and y-polarized modes as a function of (a) $d_2$ and (b) air holes layers at the wavelength of 1.55 μm.

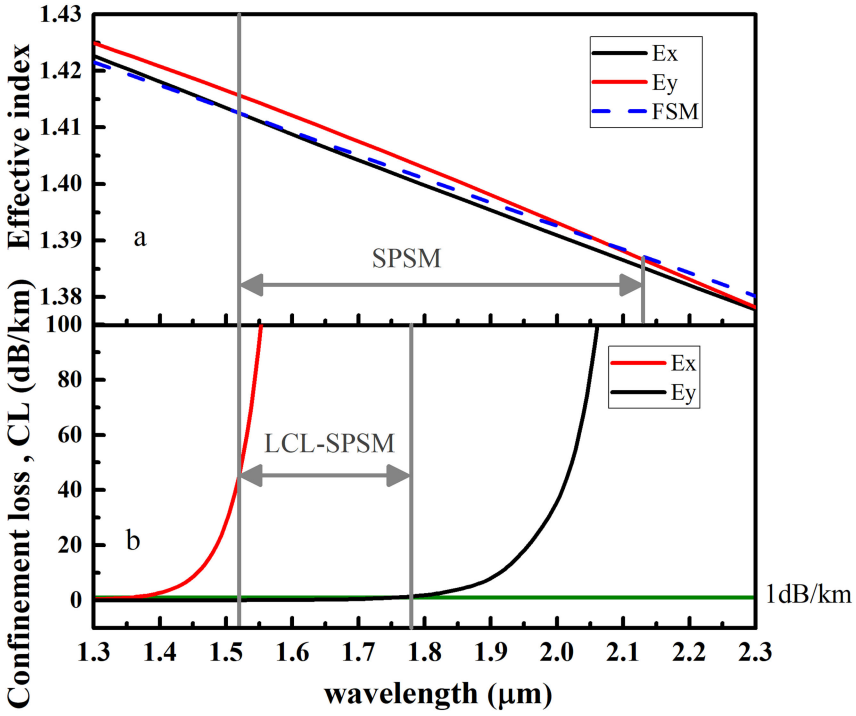


Fig. 5. Variations of the effective index (a) and confinement loss (b) with wavelengths.

with the traditional method of increasing the number of layers, our proposed design replaces the outermost air hole of the fiber with enlarged air holes, which can effectively reduce the confinement loss of the fiber and the difficulty of fabrication.

For an ideal single-polarization single-mode fiber, the cutoff wavelength of either polarization occurs when its effective index becomes equal to the cladding effective index of fundamental space-filling mode (FSM) [25]. Fig. 5(a) shows the effective index of the x- and y-polarization of the SPSM-PCF, and the cladding index of the corresponding FSM is also shown as a dotted line. The y-polarized fundamental mode has a higher effective index than the x-polarized fundamental mode, which can lead to high birefringence up to $3.25 \times 10^{-3}$ at 1.55 μm. The cutoff wavelength for x-polarization and y-polarization are 1.52 μm and 2.13 μm, respectively. Therefore, it can be realized

that the fiber experiences a single polarization operation of 610 nm bandwidth (from 1.52 μm to 2.13 μm). The variation of the confinement loss with wavelength is exhibited in Fig. 5(b). It can be found from Fig. 5(b) the bandwidth of the LCL-SPSM at 1.55 μm is from 1.52 μm to 1.78 μm.

### *3.3 Structure Deviation Tolerance on SPSM-PCF*

Similarly, this single-polarization fiber can be fabricated by the stack-and-draw method. During the fabrication process, various errors can appear, leading to the deviation of the fiber's geometrical parameters [26]. Thus, it is important to estimate the influence of fabrication errors on the fiber SPSM properties. Here, for better understanding, we insert the deviation diagram in each result figures, with dotted circulars indicating the possible fabrication errors.

*3.3.1 Effect of the Diameter Deviation on SPSM Operation:* In the actual production process, the parameters of the air holes need to be adjusted by controlling the air pressure during the drawing. However, if the air pressure is unstable, or the air holes are not well sealed [19], it will result in a slight non-uniformity in the parameters of the air holes. On the other hand, the effective refractive index of modes is mainly determined by the structure around the fiber core. So, in this section, we focus on the influence of structural parameters of air holes in the inner ring on the SPSM-band evolutions.

*(1) Variation of the Large Air Hole:* In order to distinguish the diameters between two large air holes in the core region, the diameter of the left one is defined as $D_1$ and the right one is $D_2$. Ideally, $D_1 = D_2 = 3.8$ μm. The diameter of the left large air hole $D_1$ is chosen as 3.9, 3.8, 3.7 μm, while $D_2$ and other parameters are kept constant. Fig. 6 shows the variations of effective index with the wavelength under the different diameters of the left large air hole. Comparing Fig. 6(a), (b) and (c), we can observe that the SPSM operation region moves towards the long wavelength with the decrease of the diameter of the large air hole. The reason for this phenomenon is due to the change in the core region. When the large air hole in the horizontal direction gets smaller, the curves of the effective refractive index of both orthogonal fundamental modes arise, leading to the cutoff wavelength of x- and y-polarization both moving towards the long wavelength direction.

Fig. 6(d), (e) and (f) exhibits the effect of $D_1$ on the confinement loss as a function of wavelength in the range of 1.3–2.3 μm. It is obvious that the region for LCL-SPSM operation gets narrowed severely when SPSM operation shifts to the long wavelength. According to the parameter deviation of the $D_1$, the confinement loss at 1.55 μm has changed significantly. When $D_1 = 3.7$ μm, the loss of y-polarization is up to 8.3 dB/km, no more satisfying the LCL-SPSM condition.

*(2) Variation of the Small Air Hole:* One of four small air holes in the first ring has a diameter of $d_{11}$ and $d_{11}$ is changed from 1.6 μm to 1.4 μm. Fig. 7 shows the effective index and confinement loss with the wavelength under different diameters of $d_{11}$. Similarly, both the SPSM and LCL-SPSM operation region moves towards the long wavelength direction with the decrease of small air hole, because of the rise of the effective refractive index of x-polarized mode. Comparing Fig. 6(a), (b) and (c), with Fig. 7(a), (b) and (c), the band narrowing of SPSM caused by the variation of small air hole is pronounced than that caused by large air holes. Dropping of curve of the effective refractive index of y-polarized mode is probably responsible for a tendency towards short cutoff wavelength. However, the result of LCL-SPSM operation region is completely opposite since the cutoff wavelength of LCL-SPSM in the long wavelength direction is determined by the confinement loss, indicating the variation of D induces more loss.

*3.3.2 Effect of the Position Deviation on SPSM Operation:* An SPSM-PCF perform is formed by stacking different kinds of capillary tubes around a solid rod and jacketing these stacked tubes with an outer silica tube (out-jacket tube) [18]. If the capillary deviation occurs in the stacking process, it will cause the position of air holes to deviate from the predetermined position. Therefore, it is meaningful to analyze the effect of this kind of errors on polarization stability. Corresponding to the possibility of changes in horizontal and vertical position, the impact of both two situations will be discussed. We still focus our attention on the influence of position parameters of air holes in the inner ring on the SPSM-band evolutions.

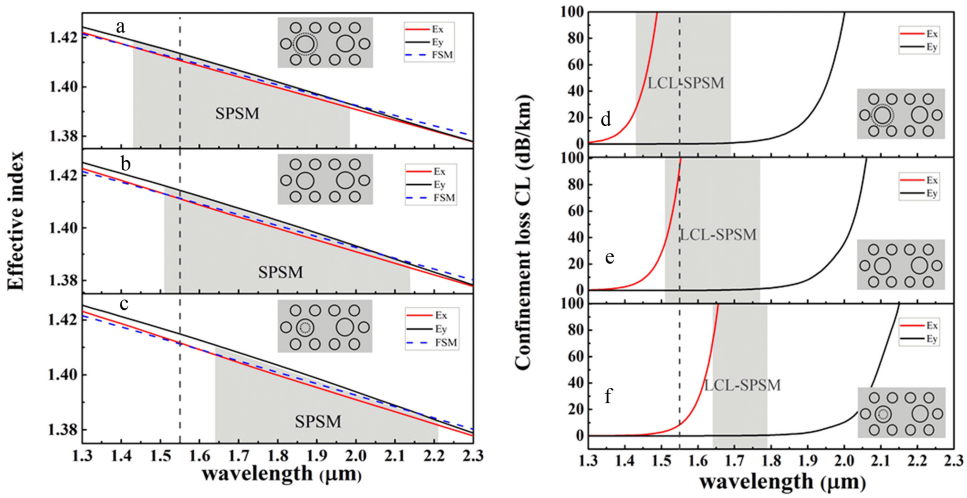


Fig. 6. SPSM and LCL-SPSM operation on different diameters of one large air hole. (a) (d) $D_1 = 3.9$ μm. (b) (e) $D_1 = 3.8$ μm. (c) (f) $D_1 = 3.7$ μm.

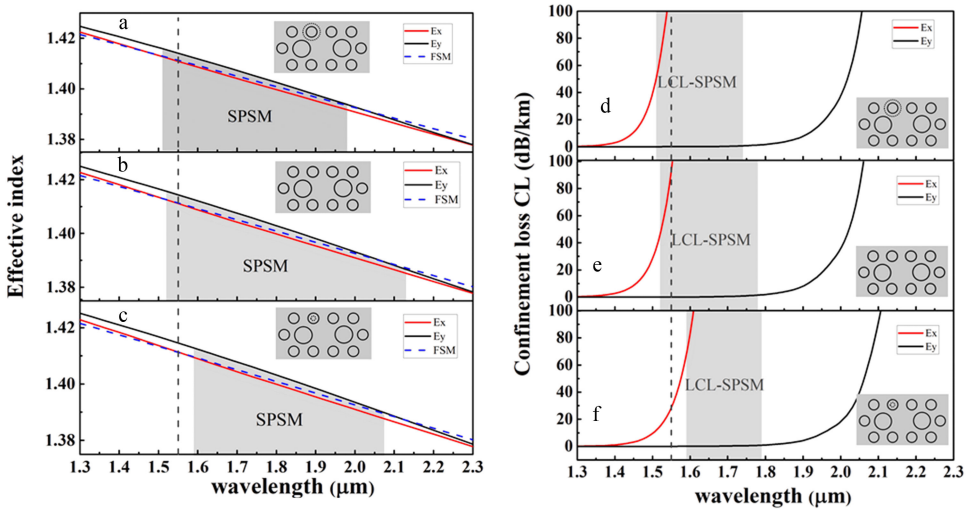


Fig. 7. SPSM and LCL-SPSM operation on different diameters of one small air hole. (a) (d) $d_{11} = 1.6$ μm. (b) (e) $d_{11} = 1.5$ μm. (c) (f) $d_{11} = 1.4$ μm.

*(1) Variation of the Large Air Hole*

*(a) Effect of the Horizontal Position Deviation of One Large Air Hole on SPSM Operation:* As described in Fig. 3, the abscissa of the left large air hole is $x_1 = -3$ μm and that of the right one is $x_2 = 3$ μm. The position of the right air hole is fixed, $x_2$ is changed from $-3.1$ μm to $-2.9$ μm and the result is shown in the Fig. 8. When $x_1 = -3.1$ μm, that is to say, when the large air hole is away from the fiber core, it induces higher effective index of all modes, and the SPSM operation moves towards long wavelength direction. In contrast, when the air hole approaches to the core, SPSM operation moves towards the short wavelength direction. What is more, the bandwidth of SPSM operation gets narrowed as long as the deviation of the horizontal position occurs. Fig. 8(d), (e) and (f), show the confinement loss with wavelength under the horizontal position deviation of the large air hole. It is realized that when $x_1 = -2.9$ μm, the SPSM operation can still be achieved at 1.55 μm. When $x_1 = -3.1$ μm, the LCL-SPSM operation band is narrowing down to 160 nm and the loss of y-polarization at 1.55 μm is too high which is easier to leak. In addition, the LCL-SPSM bandwidth decreases strongly when SPSM operation moves towards long wavelength.

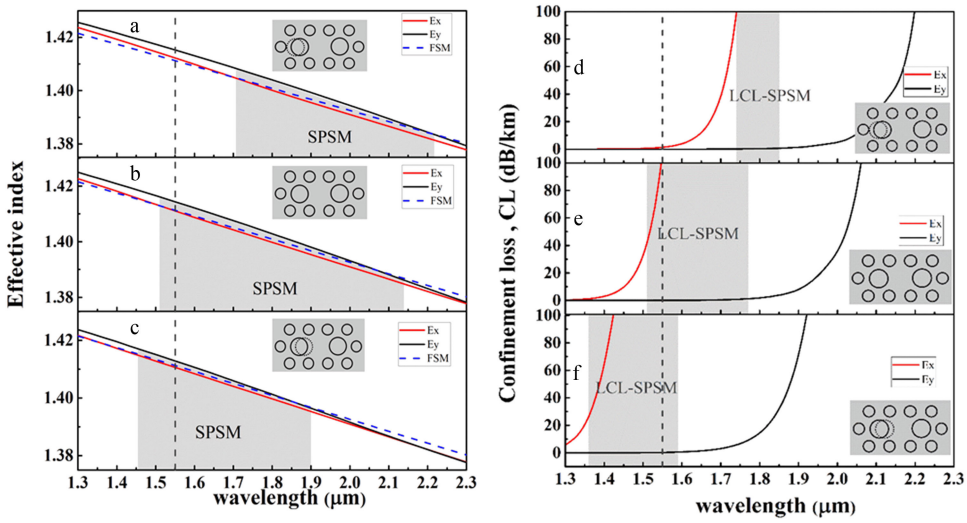


Fig. 8. SPSM and LCL-SPSM operation on different horizontal positions of one large air hole. (a) (d) $x_1 = -3.1$ μm. (b) (e) $x_1 = -3$ μm, (c) (f) $x_1 = -2.9$ μm.

TABLE 1
Polarization Property Under Different Longitudinal Positions of One Large Air Hole

| y / μm | SPSM / μm | LCL-SPSM / μm | 1.55 μm, *CL*, Ex / dB/km | 1.55 μm, *CL*, Ey / dB/km |
|---|---|---|---|---|
| 0 | 1.52-2.13 | 1.52-1.78 | 91.44 | 0.051 |
| 0.1 | 1.52-2.13 | 1.52-1.78 | 53.99 | 0.0339 |
| 0.2 | 1.52-2.13 | 1.52-1.78 | 38.04 | 0.0303 |

*(b) Effect of the Longitudinal Position Deviation of the Large Air Hole on SPSM Operation*: The ordinates of large air holes are both $y_1 = 0$ μm. Since the fiber structure is longitudinal symmetry, we merely discuss the case where the deviation is upward. The position of the right air hole is still kept constant, while $y_1$ is varied as 0, 0.1 and 0.2 μm. Table 1 shows that it almost has no effect on the SPSM and LCL-SPSM operation region, in the case of the large air hole deviating from its original position in the longitudinal direction. Compared the confinement loss at 1.55 μm under different circumstances, it should be pointed out that the proposed fiber still satisfies the LCL-SPSM condition. This phenomenon is completely different from the effect of the horizontal position deviation because this deviation has no effective impact on the distribution of the mode field.

*(2) Variation of Small Air Hole*

*(a) Effect of the Horizontal Position Deviation of One Small Air Hole on SPSM Operation:* We define the abscissa of one small air hole around core region is $x_{11}$, and change the $x_{11}$ from $-1.6$ μm to $-1.4$ μm without changing other parameters. From Fig. 9(a), (b) and (c), with $x_{11} = -1.6$, $-1.5$ and $-1.4$ μm, a cutoff of x-polarized mode occurs at 1.59, 1.52, and 1.49 μm and the cutoff of y-polarized mode occurs at 2.13, 2.13, and 1.74 μm. It indicates that the cutoff wavelength of both x- and y-polarized modes move towards short wavelength direction, which is similar to the evolution of one large air hole. As seen in the Fig. 9(d), (e) and (f), since the increase of confinement loss induced by small air holes is smaller than that of large air holes, it still can maintain a broadband LCL-SPSM operation region.

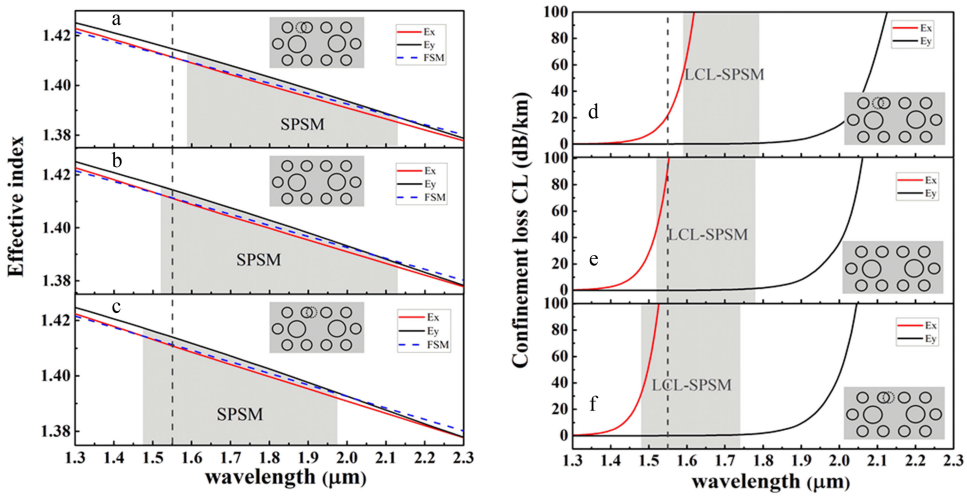


Fig. 9. SPSM and LCL-SPSM operation on different horizontal positions of one small air hole. (a) (d) $x_{11} = -1.6$ μm. (b) (e) $x_{11} = -1.5$ μm. (c) (f) $x_{11} = -1.4$ μm.

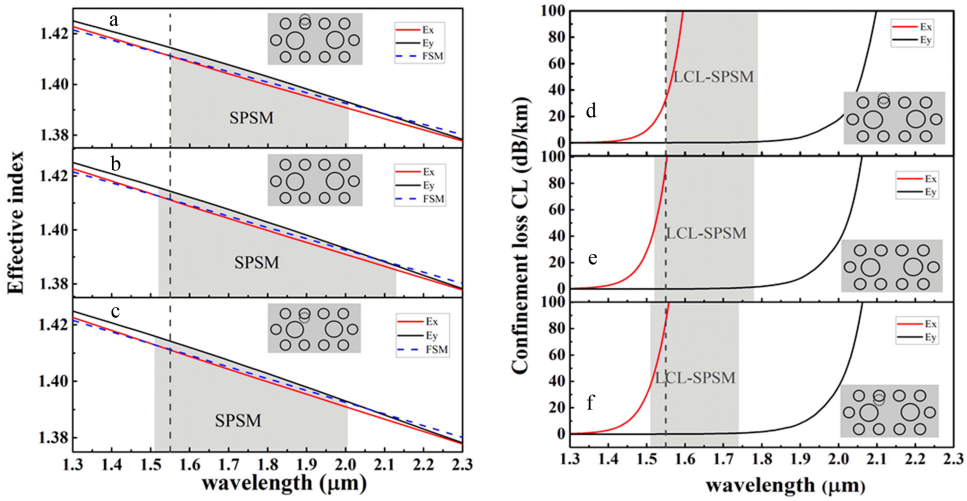


Fig. 10. SPSM and LCL-SPSM operation on the different longitudinal positions of one small air hole. (a) (d) $y_{11} = 2.698$ μm; (b) (e) $y_{11} = 2.598$ μm; (c) (f) $y_{11} = 2.498$ μm.

*(b) Effect of the Longitudinal Position Deviation of One Small Air Hole on SPSM Operation*: The ordinate of one small air hole ($y_{11}$) in the fifth ring is decreased from 2.698 μm to 2.498 μm. It can be noted that the deviation of one small air hole along the longitudinal direction still has the influence on the SPSM and LCL-SPSM bandwidths. As shown in the Fig. 10(a), (b) and (c), with $y_{11} = 2.698$, 2.598 and 2.498 μm, a corresponding SPSM operation can be realized within the wavelength range from 1.55 to 2.05 μm, 1.52 to 2.13 μm, and 1.51 to 2.05 μm, respectively. In addition, from Fig. 10(d), (e) and (f), we can know that the related LCL-SPSM operation is more or less changed. Apart from the large air hole, the longitudinal deviation induced by small air holes has a stronger impact on the SPSM and LCL-SPSM operation.

## 4. Conclusions

We have presented and analyzed a novel structure of single-polarization single-mode (SPSM) PCF. By inducing double-cladding structure, the low confinement loss bandwidth for SPSM operation of

the fundamental mode reaches 260 nm with the confinement loss low to 0.051 dB/km at 1.55 μm. The analysis of structure deviation tolerance indicates that the variations of large air hole along the x-axis have a stronger impact on the SPSM operation. Besides that, regardless of the large air hole or the small air hole, the bandwidth moves towards the same direction when the deviation trend is same except for the longitudinal. As a result, the research on structure deviation tolerance gives a significant guidance for such fiber design.

## References


[1] T. Okoshi and K. Oyamada, "Single-polarization single-mode optical fiber with refractive-index pits on both sides of core," *Electron. Lett.*, vol. 16, no. 18, pp. 712–713, 1980.

[2] H. Kubota, S. Kawanishi, S. Koyanagi, and M. Tanaka, "Absolutely single polarization photonic crystal fiber," *IEEE Photon. Technol. Lett.*, vol. 16, no. 1, pp. 182–184, Jan. 2004.

[3] H. Ma, Z. Chen, and Z. Jin, "Single-Polarization coupler based on Air-Core photonic bandgap fibers and implications for resonant fiber optic gyro," *J. Lightw. Technol.*, vol. 32, no. 1, pp. 46–54, Jan. 2014.

[4] Y. Yan, H. Ma, and Z. Jin, "Reducing polarization-fluctuation induced drift in resonant fiber optic gyro by using single-polarization fiber," *Opt. Express.*, vol. 23, no. 3, Feb. 2015, Art. no. 2002.

[5] D. Lu and J. Liu, "Broadband single-polarization single-mode operation in photonic crystal fibers with hexagonally latticed circular airholes," *J. Lightw. Technol.*, vol. 34, no. 10, pp. 2452–2458, May 2016.

[6] K. Saitoh and M. Koshiba, "Single-polarization single-mode photonic crystal fibers," *IEEE Photon. Technol. Lett.*, vol. 15, no. 10, pp. 1384–1386, Oct. 2003.

[7] M. Eguchi and Y. Tsuji, "Single-mode single-polarization holey fiber using anisotropic fundamental space-filling mode," *Opt. Lett.*, vol. 32, no. 15, Aug. 1, 2007, Art. no. 2112.

[8] P. Geng *et al.*, "Design of broadband single-polarization single-mode photonic crystal fiber based on index-matching coupling," *IEEE Photon. Technol. Lett.*, vol. 24, no. 6, pp. 452–454, Mar. 2012.

[9] S.-G. Lee, S. D. Lim, K. Lee, and S. B. Lee, "Single-polarization single-mode photonic crystal fiber based on index-matching coupling with a single silica material," *Opt. Fiber Technol.*, vol. 17, no. 1, pp. 36–40, 2011.

[10] D. Lu, X. Zhang, M. Chang, G. Wang, L. Pan, and S. Zhuang, "Endlessly single-polarization single-mode holey fibers with low confinement loss," *Opt. Lett.*, vol. 38, no. 15, pp. 2915–2918, Aug. 2013.

[11] M. Y. Chen, B. Sun, and Y. K. Zhang, "Broadband single-polarization operation in square-lattice photonic crystal fibers," *J. Lightw. Technol.*, vol. 28, no. 10, pp. 1443–1446, May 2010.

[12] T. P. White, R. C. McPhedran, C. M. d. Sterke, L. C. Botten, and M. J. Steel, "Confinement losses in microstructured optical fibers," *Opt. Lett.*, vol. 26, pp. 1660–1662, 2001.

[13] J. Ju, W. Jin, and M. S. Demokan, "Design of single-polarization single-mode photonics crystal fibers at 1.30 and 1.55," *J. Lightw. Technol.*, vol. 24, no. 2, pp. 825–830, Feb. 2006.

[14] W. Jin, Y. L. Hoo, and H. L. Ho, "Design of single-polarization PCF at 1300- and 1550-nm bands," in *Proc. SPIE*, 2004, vol. 5502, pp. 358–361.

[15] S.-G. Lee, S. D. Lim, K. Lee, and S. B. Lee, "Broadband single-polarization single-mode operation in highly birefringent photonic crystal fiber with a depressed-index core," *Jpn. J. Appl. Phys.*, vol. 49, no. 12, 2010, Art. no. 122501.

[16] A. Kumar, T. S. Saini, K. D. Naik, and R. K. Sinha, "Large-mode-area single-polarization single-mode photonic crystal fiber: design and analysis," *Appl. Opt.*, vol. 55, no. 19, Jul. 2016, Art. no. 4995.

[17] W. Zhang, S.-G. Li, Y.-J. Bao, Z.-K. Fan, and G.-W. An, "A design for single-polarization single-mode photonic crystal fiber with rectangular lattice," *Opt. Commun.*, vol. 359, pp. 448–454, 2016.

[18] T.-Y. Cho, G.-H. Kim, K.-I. Lee, S.-B. Lee, and J.-M. Jeong, "Study on the fabrication process of polarization maintaining photonic crystal fibers and their optical properties," *J. Opt. Soc. Korea.*, vol. 12, no. 1, pp. 19–24, Mar. 2008.

[19] D. M. Chow, S. R. Sandoghchi, and F. R. M. Adikan, "Fabrication of photonic crystal fibers," in *Proc. IEEE Int. Conf. Photon.*, 2012, pp. 227–230.

[20] I. H. Malitson, "Interspecimen comparison of the refractive index of fused silica," *J. Opt. Soc. Am.*, vol. 55, no. 10, pp. 1205–1209, 1965.

[21] L. Jiang, Y. Zheng, L. Hou, K. Zheng, J. Peng, and X. Zhao, "A novel ultra-broadband single polarization single mode photonic crystal fiber," *Opt. Commun.*, vol. 396, pp. 8–14, 2017.

[22] L. Wang, S. Lou, W. Chen, and H. Li, "Design of a single-polarization single-mode photonic crystal fiber with a near-Gaussian mode field and wide bandwidth," *Appl. Opt*, vol. 49, no. 32, pp. 6196–200, 2010.

[23] Y. C. Liu and Y. Lai, "Optical birefringence and polarization dependent loss of square- and rectangular-lattice holey fibers with elliptical air holes: Numerical analysis," *Opt. Express.*, vol. 13, no. 1, 2005, Art. no. 225.

[24] M. J. Messerly, J. R. Onstott, and R. C. Mikkelson, "A broadband single polarization optical fiber," *J. Lightw. Technol.*, vol. 9, no. 7, pp. 817–820, Jul. 1991.

[25] T. A. Birks, J. C. Knight, and P. S. J. Russell, "Endlessly single-mode photonic crystal fiber," *Opt. Lett.*, vol. 22, no. 13, pp. 961–963, 1997.

[26] I. A. Sukhoivanov, S. O. Iakushev, O. V. Shulika, J. A. Andrade-Lucio, A. Díez, and M. Andrés, "Supercontinuum generation at 800 nm in all-normal dispersion photonic crystal fiber," *Opt. Express.*, vol. 22, no. 24, pp. 30234–30250, Dec. 2014.